Mitogen-activated protein kinase kinase activity is required for the G_2/M transition of the cell cycle in mammalian fibroblasts

JOCELYN H. WRIGHT*†, ERLYNDA MUNAR†, DAMON R. JAMESON†, PAUL R. ANDREASSEN‡, ROBERT L. MARGOLIS‡, RONY SEGER§, AND EDWIN G. KREBS†

†Department of Pharmacology, University of Washington, Seattle, WA 98103; ‡Institut de Biologie Structurale, Jean-Pierre Ebel (Commissariat à l'Energie Atomique/Centre National de la Recherche Scientifique), 38027 Cedex 1, Grenoble, France; and §Department of Membrane Research and Biophysics, The Weitzmann Institute of Science, Rehovot 76110, Israel

ABSTRACT   The mitogen-activated protein kinase (MAPK) cascade is required for mitogenesis in somatic mammalian cells and is activated by a wide variety of oncogenic stimuli. Specific roles for this signaling module in growth were dissected by inhibiting MAPK kinase 1 (MAPKK1) activity in highly synchronized NIH 3T3 cells. In addition to the known role of this kinase in cell-cycle entry from G_0, the level of MAPKK activity was observed to affect the kinetics of progression through both the G_1 and G_2 phases of the cell cycle in NIH 3T3 cells. Ectopic expression of dominant-negative forms of MAPKK1, which was previously shown to inhibit G_0/G_1 progression, was found to also delay progression of cells through G_2. In addition, treatment of cells with the specific MAPKK inhibitor PD 98059 during a synchronous S phase arrested the cells in the following G_2 phase. These data demonstrate a novel role for the MAPK cascade in progression from G_2 into mitosis in NIH 3T3 cells.

Activation of the mitogen-activated protein kinase (MAPK) cascade is critical in the control of cellular growth by mitogenic signals in many different cell systems, including those received by tyrosine kinase, G protein-coupled and cytokine receptors, as reviewed in ref. 1. Introduction of dominant-negative forms of MAPK or MAPKK blocks quiescent cells from entering the cell cycle in response to growth factors (2–4). Activated forms of MAPKK lead to reduced dependence of cellular growth on mitogens as well as increased growth rate (3, 4) and can promote tumor growth *in vivo* (4–6).

The MAPK cascade consists of a series of serine/threonine kinases activated downstream of the small G-protein, Ras. Ras-GTP binds to and activates the serine/threonine kinase, Raf. Raf directly activates MAPKK1 and MAPKK2, which in turn activate the MAPK isoforms extracellular-regulated kinases (ERK)1 and ERK2 . On stimulation of cells with mitogens, ERK1 and ERK2, along with the downstream kinases of the ribosomal subunit kinase family, translocate to the nucleus where they phosphorylate a number of transcription factors (7). In addition to a nuclear function, MAPK has important functions in the cytoplasm. One-half of active MAPK fractionates with the microtubule cytoskeleton in cell extracts (8). Through phosphorylation of microtubule-associated proteins, MAPK regulates microtubule dynamics and other cytoskeletal changes that accompany growth (9–11). An additional pool of MAPKK1 has been shown to regulate breakdown of Golgi cisternae before cell division (12). The MAPK cascade appears to affect growth through both a nuclear function in transcriptional regulation and cytoskeletal regulated processes.

During meiosis, activation of the MAPK cascade by a germ cell-specific MAPKK activator, Mos, releases immature oocytes from a G_2 arrest and promotes a metaphase arrest in meiosis II (13, 14). The role of the MAPK cascade in the proliferation of mammalian somatic cells independent of a role in cell-cycle entry from G_0 has not been well characterized. We observed previously that ectopic expression of MAPKK1 mutants affected the growth rate of cycling cells (3). A role for the MAPK cascade in progression through the mammalian somatic cell cycle was investigated in this report by synchronizing NIH 3T3 cells and measuring the kinetics of progression through different cell-cycle phases under conditions where MAPKK activation was inhibited. In addition to a predicted role in the G_1 phase, MAPKK activity was found to be required at the G_2/M transition for the timely activation of CDC2 and progression into mitosis.

MATERIALS AND METHODS

Cell Culture. Stable cell lines were generated from NIH 3T3 cells obtained from American Type Culture Collection in 1995, as described previously (3). For synchronization, cells were plated at low density and serum starved. After 48 hr, cells were stimulated with 10% FCS and 1 μg/ml aphidicolin (Sigma). After 16–18 hr, cells were washed to remove the aphidicolin and overlaid with DMEM + 10% FCS. Experiments with PD 98059 were carried out with platelet-derived growth factor (PDGF) as a mitogen, because PD 98059 did not block MAPK activation by 10% FCS (unpublished results). Quiescent cells were stimulated with 0.2 nM PDGF and 1 μl/ml 1,000× insulin, transferrin, selenium (ITS) (GIBCO/BRL) in DMEM. In the defined medium, cells cycled through all phases more slowly than with growth in FCS. PD 98059 (Calbiochem) was added to cells from a 10 mM solution in DMSO. An equivalent volume of DMSO was added to control plates.

Fluorescence-Activated Cell Sorter (FACS) Analysis. Cells were trypsinized and fixed in 70% ethanol. Washed cells were stained with propidium iodide (PI) [4 mM sodium citrate/0.1% Triton X-100/30 units/ml DNase-free RNase A (Boehringer Mannheim)/50 μg/ml PI (Sigma)]. For MPM-2 staining, cells were fixed in 90% MeOH and incubated in a 1:750 dilution of the MPM-2 antibody followed by a 1:250 dilution of FITC-conjugated rabbit anti-mouse IgG (BioSource International, Camarillo, CA) in PBS with 3% BSA/0.05% Tween 20/2% NaN$_3$. Cells were then stained with PI as described above. The MPM-2 antibody experiments were performed in the laboratory of R. Margolis in Grenoble, and in these

---

experiments the overall cell-cycle transit time for all cell lines was faster by several hours than experiments performed in Seattle. The altered rate of growth is likely because of differences in FCS stocks between the two laboratories. All data were interpreted based on comparison of control cells analyzed in the same experiment. Analysis was done on a FAC-Scan system by using the LYSIS II program (Becton Dickinson). Histograms were prepared from the data by using REPROMAN (True Facts, Seattle, WA) or LYSIS II. The percent of cells in G_1, S, or G_2/M was quantified by DNA content by using the REPROMAN program. A cell population was recorded as being in a particular phase at time points when >50% of the cells fell within the corresponding window of PI fluorescence intensity. The kinetics of cell-cycle progression was measured in two to seven independent experiments for each clone.

MAPK Assays. Cell extracts were prepared in 50 mM β-glycero-phosphate/0.1 mM Na_3VO_4/1 mM DTT/1% Triton X-100/1 mM EGTA, pH 7.5/10 μg/ml leupeptin (United States Biochemical)/10 μg/ml aprotinin (Sigma)/2 μg/ml pepstatin A (Sigma)/1 mM each benzamidine (Sigma) and Pefabloc (Sigma). Cell lysates were fractionated by centrifugation at 14 K rpm. Supernatants were quick frozen at $-70°C$. MAPKK, and MAPK activities were measured in solution on DE-52 fractionated extracts as described previously (15). By using this method, MAPKK1 and MAPKK2 activities are measured collectively, as are those of ERK1 and ERK2. MAPK phosphorylation *in vivo* was monitored by gel mobility shift assays performed on SDS gels with an acrylamide/bisacrylamide ratio of 30:0.4 and probed with an antiserum that recognizes both ERK1 and ERK2 (3).

CDC2 Kinase Assays. Extracts were prepared as described for the MAPK assays. Cell extract (200 μg) was immunoprecipitated with anti-cyclin B antibody (no. SC-245, Santa Cruz Biotechnology) and protein A-Sepharose (Sigma). The immunoprecipitates were incubated with 4 μg histone H1 protein (Sigma) in 50 mM Tris, pH 7.5/10 mM $MnCl_2$/1 mM DTT/70 mM NaCl/10 mM γ-^{32}P-ATP (New England Nuclear) at 37°C for 30 min in an Eppendorf Thermomixer. Reactions were analyzed by SDS/PAGE and autoradiography. Relative ^{32}P-incorporation was quantified by Storage PhosphorImaging (Molecular Dynamics).

RESULTS

Expression of MAPKK Mutants Alters the Kinetics of G_2/M Progression. Ectopic expression of catalytically inactive forms of MAPKK1 generates a "dominant-negative" phenotype, interfering with activation of the endogenous enzyme. Expression of these MAPKK1 mutants in NIH 3T3 cells blocks cell from entering the cell cycle (3). Cells expressing the dominant-negative mutants also displayed slower growth rates (3). To determine when MAPKK activity was functioning in cycling cells, NIH 3T3 cell lines expressing mutant forms of MAPKK were synchronized by using a serum starvation/aphidicolin double block and examined for effects on the kinetics of cell-cycle progression. The two different dominant-negative forms of MAPKK1 used included mutation of the ATP-binding lysine (K97A) and mutation of one of the two regulatory phosphorylation sites (S222A). Cell lines expressing either wild-type or another mutant form of MAPKK1 (S222E) as well as mock-transfected cells were examined as controls. The S222E mutant behaved essentially like wild-type kinase because it still requires phosphorylation of serine 218 for activation (3).

Quiescent cells were stimulated to enter G_1 with 10% FCS. At the time of stimulation, aphidicolin was added to collect the stimulated cells at the G_1/S boundary 14 to 18 hr later. Aphidicolin binds directly to DNA polymerase and blocks DNA synthesis, while allowing for RNA and protein synthesis and progression through G_1 (16). Within 1 hr of the removal

of the aphidicolin, 80–90% of the cells commenced DNA synthesis as seen by an increase in fluorescence intensity of cells stained with PI and analyzed by FACS. Cells maintained $\geq$80% synchrony through the cell cycle (Fig. 1A).

As compared with controls, cells expressing the dominant-negative forms of MAPKK1 were delayed in G_2/M. Two or three independent clones expressing each mutant class were tested (Table 1), and FACS histograms from a representative experiment are shown in Fig. 1A. All the cell lines demonstrated similar rates of progression through S phase, except the K97A mutant expressing cells that showed a 1-hr elongation of S phase. On completion of DNA synthesis, the cells expressing either of the dominant-negative mutants maintained 4n DNA content for 2–3 hr longer than controls (Fig. 1A). These data indicate that the cells with reduced MAPKK activity had a delay in either the onset of or progression through mitosis. In contrast, overexpression of a wild-type or the S222E mutant kinase had little or no effect on the progression through G_2/M.
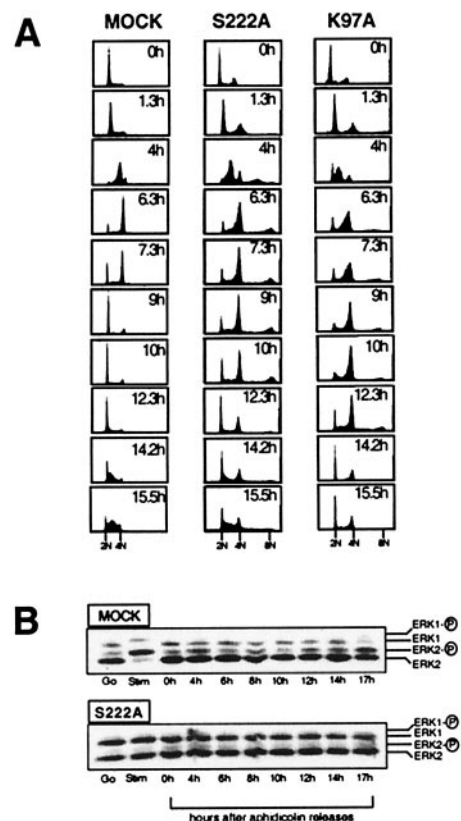

FIG. 1. Effects of ectopic expression of dominant-negative MAPKK mutants on cell-cycle progression. (*A*) FACS profiles of synchronously growing MAPKK1 mutant-expressing cells stained with PI for DNA content are shown. *A* and *B* show a profile of cells stained with PI for DNA content at a series of time points after release from an aphidicolin arrest at the G_1/S transition. At 0 hr (*Upper*), when the aphidicolin was removed, cells had 2n DNA content. As they progressed into S phase, the fluorescence intensity per cell increased (peak shifts to the right) to give >2n but <4n. At 6 hr, the majority of the cells had 4n DNA content and accumulated in a G_2/M peak. Over the next 3 hr, mock cells progressed through G_2 and M, and recovered 2N DNA content in G_1 (9 hr). By 15 hr, the mock cells had completed one cell cycle and were entering a second round of S phase. "Mock" is a cell line transfected with the pcDNA3 vector; "S222A" is a cell line transfected with the S222A-MAPKK1 mutant; "K97A" is a cell line transfected with the K97A-MAPKK1 mutant. (*B*) MAPK phosphorylation in NIH 3T3 cell lines expressing MAPKK1 mutants was measured by gel mobility shift assays of synchronized extracts from mock-transfected and S222A MAPKK-mutant transfected cell lines. The position of unphosphorylated and phosphorylated ERK1 and ERK2 are indicated to the right of each panel.

Table 1. Summary of cell-cycle kinetics of MAPKK-mutant expressing cell lines

Cell line	S phase, hr	G_2/M phase, hr	G_1 phase, hr
Mock-1	6.2 ± 0.2	3.0 ± 0.5	6.0
Mock 2	5.9 ± 0.1	3.2 ± 0.1	6.5 ± 0.5
Mock-9	5.9 ± 0.1	3.5 ± 0.1	5.9 ± 0.3
S222A-13*	6.0 ± 0.2	5.9 ± 0.1	ND
S222A-21	6.5 ± 0.3	6.2 ± 0.4	ND
K97A-2	7.0 ± 0.0	6.7 ± 0.2	ND
S222E-1	5.8 ± 0.2	3.9 ± 0.2	4.6 ± 0.3
S22E-8	$6.0^\dagger$	3.5	4.5
WT-31	6.0 ± 0.0	4.3 ± 0.3	7.0
WT-32	6.0 ± 0.0	3.7 ± 0.3	7.0

*Each clone is labeled with the letters of the mutation, followed by the cell clone number assigned in the original isolation (e.g., S222A-13). ND, not determined.

†For some clones, the timine of cell-cycle progression was measured fewer than three times and standard error could not be calculated.

Table 1 shows that similar results were obtained with multiple independently selected clones of mock-transfected controls or cells transfected with either S222A or S222E, arguing that differences were not caused simply by clonal variation.

Expression of dominant-negative mutant MAPKK1 effectively blocks mitogen stimulation of the MAPK cascade in quiescent NIH 3T3 cells (3). To determine the effect of these mutants on MAPKK activity in cycling cells, endogenous MAPKK activity in cycling cells was measured *in vivo* by monitoring endogenous ERK1 and ERK2 phosphorylation in a gel mobility shift assay of synchronized cell extracts (Fig. 1*B*). In control cells, ERK phosphorylation was detectable throughout the cell cycle, albeit at a reduced level compared with that observed in stimulated quiescent cells (Fig. 1*B* and data not shown). In comparison, the ERK phosphorylation was significantly attenuated in the cells expressing the S222A-MAPKK (Fig. 1*B*) at all time points. As part of the synchronization protocol, the cells were re-fed with fresh serum-containing media after removal of the aphidicolin. This stimulation likely contributes to the ERK phosphorylation observed in the synchronized extracts, especially at the earlier time points (Fig. 1*B*). These data are shown to demonstrate the ability of the dominant-negative MAPKK1 mutant to block all endogenous MAPKK activity throughout the cell cycle in our experimental system. In general, MAPK is active throughout G_1 and then reduces as the cells enter S phase (data not shown and ref. 46).

The delay with 4*n* DNA observed with expression of dominant-negative MAPKK mutants is consistent with either a G_2 delay and/or a mitotic delay. To distinguish between the two, cells expressing MAPKK mutants were further analyzed for the appearance of the mitosis-specific MPM-2 antigens (17). MPM-2 is an antibody with specificity toward a number of mitosis-specific protein phosphorylation sites. The reactivity of cells with this antibody increases dramatically during mitosis (17). At time points after release into S phase, synchronized S222A MAPKK-transfected cells and control cells were stained with the MPM-2 monoclonal antibody as well as with PI for DNA content. A two-parameter FACS analysis allowed simultaneous assessment of DNA content and level of MPM-2 antigens for each cell (Fig. 2*A*). Fig. 2*B* graphically illustrates the percent of cells that were MPM-2-positive as a function of time in two experiments, Fig. 2*B Left* corresponding to the data in Fig. 2*A*. The mock-transfected cell line peaked in MPM-2 reactivity at 6.5 hr after release, whereas the dominant-negative S222A mutant peaked in MPM-2 signal at 8 hr. In an additional experiment (Fig. 2*B Right*), the S222E mutant, which showed normal G_2/M kinetics by PI staining (Table 1),
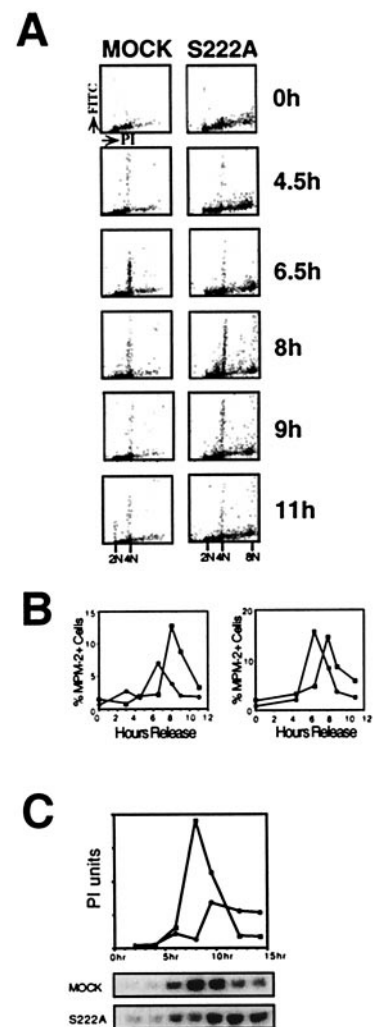

FIG. 2. MAPKK mutants delay the G_2/M transition as seen by MPM-2 antibody reactivity and CDC2 activation in synchronized cells. (*A*) Two-dimensional FACS analysis of cells stained with PI and MPM-2 antibody/FITC secondary antibody were compared from mock and MAPKK-S222A mutant transfected cell lines. Dot plots show the relative PI fluorescence intensity (*x* axis; linear) vs. the relative FITC/MPM-2 fluorescence intensity (*y* axis; logarithmic) for the two cell lines at different time points. A representative data set is shown. (*B*) The relative FITC fluorescence is plotted vs. time from two data sets, one from the data set above (*Left*) comparing mock-transfected (black circles) and MAPKK S222A mutant-expressing (white squares) cell lines. MAPKK S222E (black squares) and S222A dominant-negative (white squares) MAPKK mutant-expressing cell lines are compared (*Right*). (*C*) Comparison of the timing and magnitude of CDC2 activation in MAPKK S222A mutant and mock-transfected cell lines. Autoradiograms of SDS/PAGE analyses of phosphorylated histone H1 and PhosphorImager (PI) quantification of the gels are shown. The *x* axis is time after release of cells into S phase.

also peaked in MPM-2 signal at 6.5 hr, whereas the S222A mutant again showed delayed appearance of MPM-2 antigens. These results suggest that the dominant-negative mutant-expressing cells were delayed in G_2. Further evidence that cells were delayed in G_2 is that S222A mutant cells had a spread morphology and intact nuclear envelopes at 6.5 hr after release, whereas controls had peak populations of rounded cells without intact nuclei (data not shown).

The interphase-mitosis transition is triggered by the activation of the cyclin B-CDC2 kinase complex. Comparison of mock- and S222A-transfected cell lines revealed that the peak of CDC2 kinase activity in the S222A mutant was both

attenuated and delayed by 2–3 hr (Fig. 2C). These data suggest that MAPKK activity was required for activation of CDC2 in G_2, and the delay in progression into mitosis in the MAPKK-mutant expressing cells is a result of stalling CDC2 activation.

MAPKK Mutant Cells Develop a Tetraploid Subpopulation. Another phenotype observed with the MAPKK overexpressing cell lines was that 10–30% of the cells were tetraploid, depending on the clone. Tetraploidy was observed as a subset of synchronized cells that had twice the DNA fluorescence intensity at all time points, cycling between $4n$ and $8n$ DNA content (Figs. 1A and 2A). The possibility that these cells represented cell–cell doublets was excluded by "gating" to include only single cells during collection of the FACS data. A defect in cytokinesis, as determined by the presence of binucleate cells, was ruled out by microscopic examination of PI-stained cells (data not shown). The generation of tetraploid cells is presumably caused by the cells undergoing two rounds DNA synthesis without mitosis or by failure of chromosome segregation in mitosis. A tetraploid subpopulation of cells was observed in seven of seven MAPKK mutant-expressing cell lines, but in only one of four mock-transfected cell lines. When a single cell cycle was examined in mutant cells as shown in Fig. 1, no measurable increases in ploidy were observed in the FACS analysis of PI-stained cells. This indicates that the incidence of mitotic bypass or failure was low, and that the significant percent of tetraploid cells was likely because of accumulation of events over multiple cell divisions during selection of the clonal cell lines.

The MAPKK Inhibitor PD 98059 Causes a G_2 Arrest in Synchronously Growing Cells. The G_2 delay observed in the MAPKK mutant cells suggests that MAPKK activity is required for some aspect of G_2 progression into mitosis. An inhibitor of MAPKK was added to synchronized NIH 3T3 cells late in S phase to test whether the kinase activity was specifically required during G_2 as opposed to an indirect effect caused by a deficiency in essential G_2 factors synthesized earlier in the cell cycle. The drug PD 98059 has been shown to specifically block the activation of MAPKK1 and MAPKK2 *in vivo* (18). This drug was relatively inactive in high serum (unpublished data), so the effects of PD 98059 on cell-cycle progression were assessed in cells grown in a defined medium with PDGF rather than whole serum as a mitogen.

Cells were synchronized with a serum starvation/aphidicolin double block and stimulated with PDGF to enter the cell cycle. PD 98059 was added 8 hr after release into S phase and cell-cycle progression was followed for 30 hr (Fig. 3A). At 20 hr after release into S phase, the control cells had completed mitosis and returned to G_1, whereas all of the cells treated with PD 98059 were arrested in G_2 with $4n$ DNA content. The arrested cells maintained the flat morphology and intact nuclear envelope characteristic of interphase cells (microscopic data not shown). Drug-treated cells remained blocked with $4n$ DNA content for an additional 10 hr, with only 30% of the cells successfully completing mitosis and reentering G_1 by the 30-hr time point. The subset of cells that reentered G1 either eventually acquired the ability to undergo mitosis in the absence of MAPKK activity, or the active concentration of the PD 98059 fell below a threshold level allowing sufficient MAPKK to be activated in these cells. The latter possibility is supported by our observation that PD 98059 only poorly inhibits MAPKK activation by growth factors when the drug is added 16 hr before stimulation, as compared with 30 min before stimulation (J. S. Campbell and J.H.W., unpublished results). With either explanation, the block induced by the drug appears to be reversible. When CDC2-cyclin B activation was measured in synchronized cell extracts prepared from cells treated with the drug in late S phase, PD 98059 significantly reduced the activation of CDC2 as compared with the DMSO control (Fig. 3B).
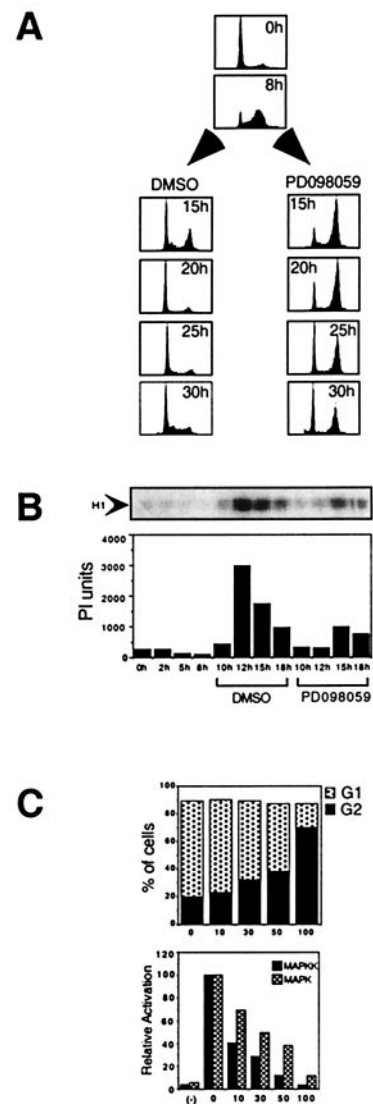

FIG. 3. The effect of PD 98059 on G_2 progression. (A) Quiescent cells were stimulated with PDGF in the presence of aphidicolin for 20 hr. Cells were released into S phase (0 hr). During late S phase (8 hr), 100 μM PD 98059/DMSO or DMSO alone were added to the cells. At 15, 20, 25, and 30 hr after release, cells were stained with PI for DNA content and analyzed by FACS. (B) The effect of addition of 100 μM PD 98059 to late S phase cells on the subsequent activation of cyclin B-CDC2 complexes. The PD 98059 or DMSO vehicle control was added at the 8-hr time point shown. An autoradiogram of phosphorylated histone H1 is shown. PhosphorImager quantification of the gel is shown graphically below. (C) Comparison of the dose required for kinase inhibition and for the G_2 delay. The upper graph shown the percent of cells in G_1 (stacked gray bars) and G_2 (black bars) as a function of drug concentration 1n micromoles per liter. The PD 98059 was added in late S phase (8 hr), and cells were collected and stained at the 20-hr time point as shown in A. The lower graph shows the relative activity of MAPK and MAPKK as a function of the dose of PD 98059. Quiescent NIH 3T3 cells were treated with the indicated concentration of PD 98059 or DMSO vehicle alone 30 min before stimulation with 0.2 nM PDGF for 3 min. MAPKK activity (black bars) was measured by using a coupled assay with ERK2 as substrate. MAPK activity (gray bars) was measured by using myelin basic protein as substrate.

The dose response for the arrest of cells in G_2 by PD 98059 was compared with the dose response for drug inhibition of MAPKK and MAPK activation by PDGF. Various doses of PD 98059 were added to synchronized S phase cells, and the percentage of cells in G_2 vs. G_1 was assessed at 20 hr after release. Both G_2 progression (Fig. 3C Upper) and activation of

MAPKK and MAPK (Fig. 3*C Lower*) were inhibited in a dose-responsive manner. The doses required for inhibition of the kinases and for G_2 progression were comparable. PD 98059 (100 μM) blocked MAPKK and MAPK activation completely and caused significant cell cycle arrest in G_2. At PD 98059 concentrations of 30 and 50 μM, MAPKK activation was still significantly blocked, yet MAPK activation was only 50% inhibited and only a slight delay in G_2 was observed (Fig. 3*C*). The equivalence of the dose responses is consistent with PD 98059 blocking cells in G_2 as a result of blocking MAPK activation. To rule out the possibility of any artifactual requirement for MAPKK activity in G_2 as a result of holding the cells at the G_1/S boundary, quiescent cells were stimulated with PDGF in the absence of aphidicolin. PD 98059 was added 20 hr later after all the cells had entered the cell cycle (PD 98059 treatment will block the cells from entering the cycle if added with mitogen) (19). Even in the absence of an aphidicolin arrest, 100 μM PD 98059 still caused a dramatic G_2 arrest (Fig. 4).

In parallel experiments, PD 98059 was added to synchronized cells in early G_1 at 17 hr after aphidicolin release. Under these conditions, MAPKK inhibition arrested postmitotic cells in G_1 (data not shown). This result was anticipated based on the fact that MAPKK has been shown to be required for the G_0/G_1–S transition (3). Together, these data indicate that MAPKK activity is required for both the G_2/M and G_1/S transitions in actively cycling NIH 3T3 cells.

DISCUSSION

It has previously been established that activation of MAPK cascade is essential for entry into the somatic cell cycle in response to mitogens. A careful analysis of synchronized cells has revealed that the MAPK cascade functions not only in the G_0/G_1– S transition but also in the transition from G_2 to M in NIH 3T3 cells. Initially, we expected our previously published reduction in growth rate of cells expressing dominant-negative MAPKK mutants (3) to be explained by cells having a longer G_1 phase or a greater propensity to exit the cell cycle after mitosis. Instead the slower growth in these cells was linked to a delay in G_2/M progression in multiple independent clones. Cells were delayed either in G_2 or early prophase by the criterion that cells remained longer with $4n$ DNA content, but before nuclear envelope breakdown, CDC2 activation, and MPM-2 epitope phosphorylation. This result is in accord with evidence for a G_2/M function of two oncogenes that activate the MAPK cascade, Src and Raf, reviewed in ref. 20.

The ability of the MAPKK inhibitor PD 98059 added in late S phase to block the following G_2/M transition corroborates results obtained with the mutant cells. It also indicates that MAPKK activity was required directly during these latter phases of the cell cycle rather than being required earlier for expression of a protein that functions later at the G_2/M transition. Although PD 98059 has been shown to be a specific inhibitor of MAPKK (not inhibiting other kinases) (18), it has recently been found to be a potent inhibitor of cyclooxygenase
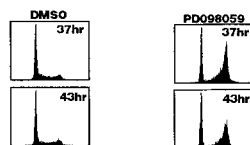

FIG. 4. The effect of PD 98059 on cell-cycle progression in the absence of aphidicolin treatment. Cells were plated at low density and grown in low serum for 48 hr. PDGF was added to induce them to enter the cell cycle. After 20 hr, when the cells had all entered the cell cycle, PD 98059 was added to 100 μM or an equivalent volume of DMSO. Cells were collected and stained with PI for FACS at 37 and 43 hr after serum stimulation.

(21). This alternative activity of PD 98059 is not likely to be responsible for the G_2 arrest, because the doses of drug required to inhibit both MAPK activation and G_2 progression were similar, whereas the dose required for cyclooxygenase inhibition is two orders of magnitude lower than was required for G_2 arrest (21).

In *Xenopus* oocytes, the MAPK cascade plays an essential role in the onset of meiosis I during meiotic maturation (22–24) in response to synthesis of the germ cell-specific MAPKK activator Mos. Data presented here are the first evidence that MAPKK functions in the onset of mitosis in somatic cells where Mos is not expressed (13). Our results in fibroblasts are also in marked contrast to cycling embryonic extracts from *Xenopus*, where MAPK activity is not required for mitotic entry (25) and can even inhibit mitotic entry when inappropriately activated (26, 27, 47). These early mitotic cycles differ from somatic cell cycles in that they are very rapid and lack G_1 and G_2 phases (28). Likely MAPKK functions in a somatic cell G_2 checkpoint that is absent during embryogenesis. There are multiple checkpoints in somatic cells during G_2 or early prophase before nuclear envelope breakdown such as those that sense DNA damage or incomplete DNA replication and decatenation, reviewed in ref. 29. Interestingly, a *Schizosaccharomyces pombe* MAPKK homologue, WIS1, has been shown to function as a dose-dependent inducer of mitosis (30). In mammalian cells, MAPKK2 has been implicated in recovery from a DNA damage-induced G_2 arrest (48). Because 100 μM PD 98059 blocks both MAPKK1 and MAPKK2 activation (18), the G_2 block we observed when cells are drug treated in S phase may relate to this DNA damage-induced checkpoint.

The G_2/M phase transition is triggered by the activation of the CDC2-cyclin B kinase complex (31, 32). CDC2-cyclin B kinase activation in G_2 was delayed in the dominant-negative MAPKK-expressing cell lines and was also blocked by addition of PD 98059 to S phase cells, indicating that MAPKK activity was required for the activation of CDC2 at the G_2/M transition. The CDC2 kinase is regulated by multiple factors, which culminate in the rapid dephosphorylation of CDC2 and activation of the CDC2-cyclin B complex at the G_2/M transition (33). Cyclin B protein levels are cell-cycle regulated, with the protein synthesized *de novo* each cell cycle (34). In data not shown, Western blots probed with anti-cyclin B revealed no decrease in cyclin B levels in the same synchronized extracts from MAPKK dominant-negative mutant-expressing cells that were delayed in CDC2 activation. Thus a deficiency of cyclin B was not responsible for the observed G_2 delay in the mutant cells.

Myt1 is a major protein kinase activity in somatic cells that keeps cyclin B-CDC2 complexes inactive through phosphorylation during S and G_2 phases (35). The MAPK-regulated kinase ribosomal subunit kinase phosphorylates and inactivates Myt1 (36). MAPK inhibition could therefore increase Myt1 activity and prevent CDC2 activation. MAPK could also regulate CDC2 through phosphorylation of cyclin B. Cyclin B is a substrate for MAPK (37), and phosphorylation of cyclin B on MAPK sites is important for translocation of the complex to the nucleus, where it is activated by CDC25C (38). MAPK may also regulate CDC2 activation indirectly through regulation of microtubule networks where the CDC2-cyclin B complex is localized (39). MAPK plays an essential role in spindle formation (40), and MAPKK1 is required for Golgi fragmentation (12), providing two important cytoplasmic functions for these kinases in the G_2/M transition. MAPKK function at G_2/M may also be nuclear given a recent report showing striking translocation of MAPKK1 to the nucleus during early prophase (41).

In addition to the effect on cell-cycle kinetics, overexpression of MAPKK1 mutants induced tetraploidy in a subpopulation of cells, indicating that these cells bypassed mitosis or

failed in chromosome segregation with some frequency. Unlike the G_2 delay, the tetraploidy developed in cell lines ectopically expressing all forms of MAPKK1, both active and inactive. MAPK likely has multiple roles in mitosis and needs to be correctly activated and inactivated for normal mitotic progression. Indeed, it was shown in *Xenopus* that the level of MAPK activity affects the duration of mitosis (40). In the recent report from Abbott and Holt discussed above (48), it is interesting to note that a fraction of their MAPKK1-mutant cells developed a new peak of 8n DNA after recovery from ionizing radiation. This indicates that, although they show that MAPKK2 is required for recovery from the arrest, MAPKK1 may be important to prevent cells from bypassing mitosis after DNA damage. The observation that a pool of active MAPK localizes to kinetochores in mammalian cells suggests that MAPK may play a direct positive role in chromosome segregation (42, 43). A role for the MAPK cascade in mitotic fidelity is supported by a pronounced decrease in chromosome stability with deregulation of activators of the MAPK cascade (44, 45).

The MAPK cascade has been extensively studied in the stimulation of quiescent cells with mitogenic factors and is generally considered to be an important factor in the initiation of growth or mitogenesis. We have investigated the role for the MAPK cascade in actively growing cells by examining interactions between MAPKK activity and different cell-cycle phases by using synchronized NIH 3T3 cells. Results presented here demonstrate that this cascade not only promotes growth through mitogenic signaling to enter the cell cycle, but also functions in putative signal transduction pathways required for progression through the G_1 and G_2 phases of the cell cycle in actively cycling fibroblasts.

1. Robinson, M. J. & Cobb, M. H. (1997) *Curr. Opin. Cell Biol.* **9,** 180–186.
2. Pages, G., Lenormand, P., L'Allemain, G., Chambard, J. C., Meloche, S. & Pouyssegur, J. (1993) *Proc. Natl. Acad. Sci. USA* **90,** 8319–8323.
3. Seger, R., Seger, D., Reszka, A. A., Munar, E. S., Eldar Finkelman, H., Dobrowolska, G., Jensen, A. M., Campbell, J. S., Fischer, E. H. & Krebs, E. G. (1994) *J. Biol. Chem.* **269,** 25699–25709.
4. Brunet, A., Pages, G. & Pouyssegur, J. (1994) *Oncogene* **9,** 3379–3387.
5. Mansour, S. J., Matten, W. T., Hermann, A. S., Candia, J. M., Rong, S., Fukasawa, K., Vande Woude, G. F. & Ahn, N. G. (1994) *Science* **265,** 966–970.
6. Cowley, S., Paterson, H., Kemp, P. & Marshall, C. J. (1994) *Cell* **77,** 841–852.
7. Treisman, R. (1996) *Curr. Opin. Cell Biol.* **8,** 205–215.
8. Reszka, A. A., Seger, R., Diltz, C. D., Krebs, E. G. & Fischer, E. H. (1995) *Proc. Natl. Acad. Sci. USA* **92,** 8881–8885.
9. Reszka, A. A., Bulinski, J. C., Krebs, E. G. & Fischer, E. H. (1997) *Mol. Biol. Cell* **8,** 1219–1232.
10. Gotoh, Y., Nishida, E., Matsuda, S., Shiina, N., Kosako, H., Shiokawa, K., Akiyama, T., Ohta, K. & Sakai, H. (1991) *Nature (London)* **349,** 251–254.
11. Lovric, J., Dammeier, S., Kieser, A., Mischak, H. & Kolch, W. (1998) *J. Biol. Chem.* **273,** 22848–22855.
12. Acharya, U., Mallabiabarrena, A., Acharya, J. K. & Malhotra, V. (1998) *Cell* **92,** 183–192.
13. Sagata, N. (1997) *BioEssays* **19,** 13–21.
14. Gebauer, F. & Richter, J. D. (1997) *BioEssays* **19,** 23–28.
15. Ahn, N. G., Weiel, J. E., Chan, C. P. & Krebs, E. G. (1990) *J. Biol. Chem.* **265,** 11487–11494.
16. Pedrali Noy, G., Spadari, S., Miller Faures, A., Miller, A. O., Kruppa, J. & Koch, G. (1980) *Nucleic Acids Res.* **8,** 377–387.
17. Davis, F. M., Tsao, T. Y., Fowler, S. K. & Rao, P. N. (1983) *Proc. Natl. Acad. Sci. USA* **80,** 2926–2930.
18. Alessi, D. R., Cuenda, A., Cohen, P., Dudley, D. T. & Saltiel, A. R. (1995) *J. Biol. Chem.* **270,** 27489–94.
19. Dudley, D. T., Pang, L., Decker, S. J., Bridges, A. J. & Saltiel, A. R. (1995) *Proc. Natl. Acad. Sci. USA* **92,** 7686–7689.
20. Laird, A. D. & Shalloway, D. (1997) *Cell. Signal.* **9,** 249–255.
21. Borsch-Haubold, A. G., Pasquet, S. & Watson, S. P. (1998) *J. Biol. Chem.* **273,** 28766–28772.
22. Gotoh, Y., Masuyama, N., Dell, K., Shirakabe, K. & Nishida, E. (1995) *J. Biol. Chem.* **270,** 25898–258904.
23. Haccard, O., Lewellyn, A., Hartley, R. S., Erikson, E. & Maller, J. L. (1995) *Dev. Biol.* **168,** 677–682.
24. Kosako, H., Gotoh, Y. & Nishida, E. (1994) *EMBO J.* **13,** 2131–2138.
25. Takenaka, K., Gotoh, Y. & Nishida, E. (1997) *J. Cell Biol.* **136,** 1091–1097.
26. Abrieu, A., Fisher, D., Simon, M.-N., Doree, M. & Picard, A. (1997) *EMBO J.* **16,** 6407–6413.
27. Walter, S. A., Guadagno, T. M. & Ferrell, J. E. J. (1997) *Mol. Biol. Cell* **8,** 2157–2169.
28. Gerhart, J. C. (1980) in *Mechanisms Regulating Pattern Formation in the Amphibian Egg and Early Embryo*, ed. Goldberger, R. F. (Plenum, New York), Vol. 2, pp. 133–316.
29. Elledge, S. J. (1996) *Science* **274,** 1664–1668.
30. Warbrick, E. & Fantes, P. A. (1991) *EMBO J.* **10,** 4291–4299.
31. Riabowol, K., Draetta, G., Brizuela, L., Vandre, D. & Beach, D. (1989) *Cell* **57,** 393–401.
32. Th'ng, J. P., Wright, P. S., Hamaguchi, J., Lee, M. G., Norbury, C. J., Nurse, P. & Bradbury, E. M. (1990) *Cell* **63,** 313–324.
33. Morgan, D. O. (1995) *Nature (London)* **374,** 131–134.
34. Sherr, C. J. (1996) *Science* **274,** 1672–1677.
35. Liu, F., Stanton, J. j., Wu, Z. & Piwnica-Worms, H. (1997) *Mol. Cell Biol.* **17,** 571–583.
36. Palmer, A., Gavin, A.-C. & Nebreda, A. R. (1998) *EMBO J.* **17,** 5037–5047.
37. Izumi, T. & Maller, J. L. (1991) *Mol. Cell Biol.* **11,** 3860–3867.
38. Li, J., Meyer, A. N. & Donoghue, D. J. (1997) *Proc. Natl. Acad. Sci. USA* **94,** 502–507.
39. Ookata, K., Hisanaga, S., Bulinski, J. C., Murofushi, H., Aizawa, H., Itoh, T. J., Hotani, H., Okumura, E., Tachibana, K. & Kishimoto, T. (1995) *J. Cell Biol.* **128,** 849–862.
40. Guadagno, T. M. & Ferrell, J. E., Jr. (1998) *Science* **282,** 1312–1315.
41. Tolwinski, N. S., Shapiro, P. S., Goueli, S. & Ahn, N. G. (1999) *J. Biol. Chem.* **274,** 6168–6174.
42. Zecevic, M., Catling, A. D., Eblen, S. T., Renzi, L., Hittle, J. C., Yen, T. J., Gorbsky, G. J. & Weber, M. J. (1998) *J. Cell Biol.* **142,** 1547–1558.
43. Shapiro, P. S., Vaisberg, E., Hunt, A. J., Tolwinski, N. S., Whalen, A. M., McIntosh, J. R. & Ahn, N. G. (1998) *J. Cell Biol.* **142,** 1533–1545.
44. Denko, N. C., Giaccia, A. J., Stringer, J. R. & Stambrook, P. J. (1994) *Proc. Natl. Acad. Sci. USA* **91,** 5124–5128.
45. Fukasawa, K. & Vande Woude, G. F. (1997) *Mol. Cell. Biol.* **17,** 506–518.
46. Meloche, S. (1995) *J. Cell. Physiol.* **163,** 577–588.
47. Bitangcol, J. C., Chau, A. S., Stadnick, E., Lohka, M. J., Dicken, B. & Shibuya, E. K. (1998) *Mol. Biol. Cell* **9,** 451–467.
48. Abbott, D. W. & Holt, J. T. (1999) *J. Biol. Chem.* **274,** 2732–2742.